CrystEngComm

RSC Publishing

COMMUNICATION

View Article Online
View Journal | View Issue

Syntheses, structures, and photoluminescent properties of a series of zinc(II)–3-amino-1,2,4-triazolate coordination polymers constructed by varying carboxylate anions†

Cite this: *CrystEngComm*, 2013, **15**, 3261

Received 10th January 2013,
Accepted 14th February 2013

DOI: 10.1039/c3ce00049d

www.rsc.org/crystengcomm

JinYing Gao,[a] Ning Wang,[b] XiaHua Xiong,[c] ChuJun Chen,[a] WeiPing Xie,[a] XingRui Ran,[a] Yi Long,[b] ShanTang Yue*[a] and YingLiang Liu[d]

To explore the influence of different carboxylate ligands on the structures of metal–organic frameworks (MOFs), five novel Zn(II) coordination polymer compounds, namely, $\{[Zn(atz)(bia)]\}_n$ (1), $\{[Zn_3(atz)_3(tpa)_{3/2}]\}_n$ (2), $\{[Zn_2(atz)_2(pda)]\}_n$ (3), $\{[Zn_4(atz)_2(btc)]\cdot 4H_2O\}_n$ (4) and $\{[Zn_2(atz)_2(btec)]\cdot H_2O\}_n$ (5) have been successfully obtained by introducing various secondary auxiliary ligands in Zn(II)–L systems, characterized by elemental analysis, FT-IR, thermogravimetric analysis (TGA), powder X-ray diffraction (PXRD) and single-crystal X-ray diffraction (Hatz = 3-amino-1,2,4-triazolate, Hbia = benzoic acid, H_2tpa = 1,4-terephthalic acid, H_2pda = 1,4-benzenediacetic acid, H_3btc = 1,3,5-benzenetricarboxylate, H_4btec = 1,2,4,5-benzenetetracarboxylic). Compound 1 features a 2D layer with (4.8^2) topology, which is further stabilized by hydrogen bonds between the uncoordinated amino groups and uncoordinated oxygen atoms from bia ligands. Compound 2 exhibits a 3D 3,4-connected framework with $\{4.8^2.10^3\}\{4.8^2\}$ topology, constructed from Zn(II) ions and μ_3-atz ligand. Compound 3 displays a 3D 3,4-connected network with $\{4.6.8\}\{4.6^2.8^3\}$ topology. Compound 4 possesses a 3D 9-nodal network with a point symbol of $\{4.8.9\}_2\{4.8^2\}\{4.8^3.9.10\}\{5.8.9\}_4\{5.8^2\}$. Compound 5 shows a 3D 3,4,4-connected framework with $\{4.8^2\}_4\{4^2.8^3.10\}_2\{8^4.10^2\}$ topology. The diverse structures of these five complexes demonstrate that the skeleton of carboxylate ligands have a significant impact on the construction of MOFs. Moreover, the luminescence properties of complexes 1–5 were investigated in the solid state.

Introduction

Rational design and successful construction of metal–organic frameworks (MOFs) has undergone tremendous development in recent years owing to their intriguing variety of architectures and captivating topologies as well as their potentially multi-field applications in magnetism, gas storage, luminescence and catalysis.[1–6] The rapid development of MOFs with versatile structures and desired properties is inevitable to involve appropriate organic ligands which play a key role in directing the ultimate complex architectures. In addition, the solvent system, molar ratio of reactants, pH values, temperature and metal ions also influence the final architectures.[7] Up to now, many studies focused on the use of O or N-donor organic molecules and a large number of rigid ligands have been employed extensively in constructing functional coordination polymers because they exhibit flexible coordination modes and afford more predictable coordination modes, such as pyrazole, imidazole, tetrazole, and so on.[8] However, reports of MOFs constructed from tridentate ligands are relatively rare.[9] 1H-1,2,4-triazole and its derivatives which unite the coordination geometries of both pyrazole and imidazole have attracted growing interest in coordination chemistry because of the fact that the triazole ring with strong σ-donor and weak π-acceptor properties as well as their potential $\mu_{1,2}$-, $\mu_{2,4}$- and $\mu_{1,2,4}$-bridging fashions.

On the other hand, as an important family of multidentate O-donor ligands, polycarboxylate organic ligands have been witnessed to be excellent structural constructors due to their various coordination modes to metal ions.[10] The employment of mixed ligands of polycarboxylates, which would cause the structural diversity and construct interesting topologies.[11] Moreover, a systematic investigation of the influence of different aromatic carboxylates on the structures is valuable. Taking all of the above into account, by introducing five aromatic carboxylate ligands with different geometric shapes (Chart 1) as auxiliary ligands into the Zn(II)–atz synthesis system (Scheme 1), a series of novel MOFs with different structures and dimensionalities, namely, $\{[Zn(atz)(bia)]\}_n$ (**1**), $\{[Zn_3(atz)_3(tpa)_{3/2}]\}_n$ (**2**), $\{[Zn_2(atz)_2(pda)]\}_n$ (**3**), $\{[Zn_4(atz)_2(btc)]\cdot 4H_2O\}_n$ (**4**)

[a]*School of Chemistry and Environment, South China Normal University, Guangzhou 510006, P. R. China. E-mail: yuesht@scnu.edu.cn; Fax: +86 20 39310187; Tel: +86 20 39310187*

[b]*School of Materials Science and Engineering, Nanyang Technological University, 50 Nanyang Avenue, 639798, Singapore*

[c]*College of Material Science of Engineering, South China University of Technology, Guangzhou, 510640, P. R. China*

[d]*College of Science, South China Agricultural University, Guangzhou 510642, P. R. China*

† Electronic supplementary information (ESI) available: Contain the supplementary crystallographic data for **1–5**. PXRD patterns, table of selected bond distances and angles for **1–5**, the FTIR spectra figures for **1–5**. CCDC 917345–917349. For ESI and crystallographic data in CIF or other electronic format see DOI: 10.1039/c3ce00049d

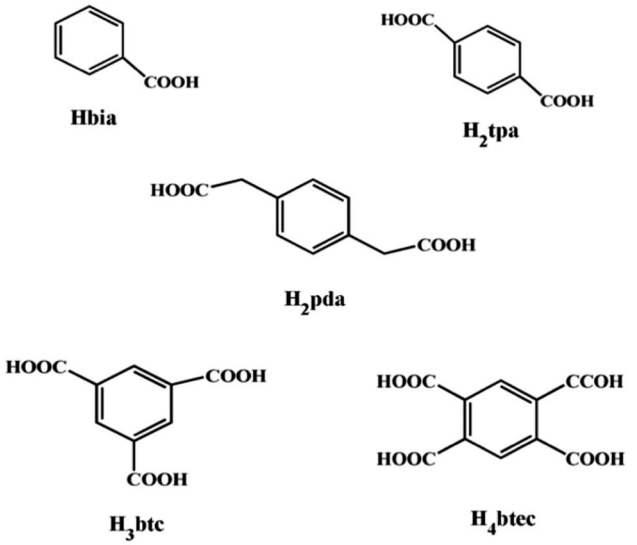

Chart 1 Structures of the carboxylate ligands used in this work.

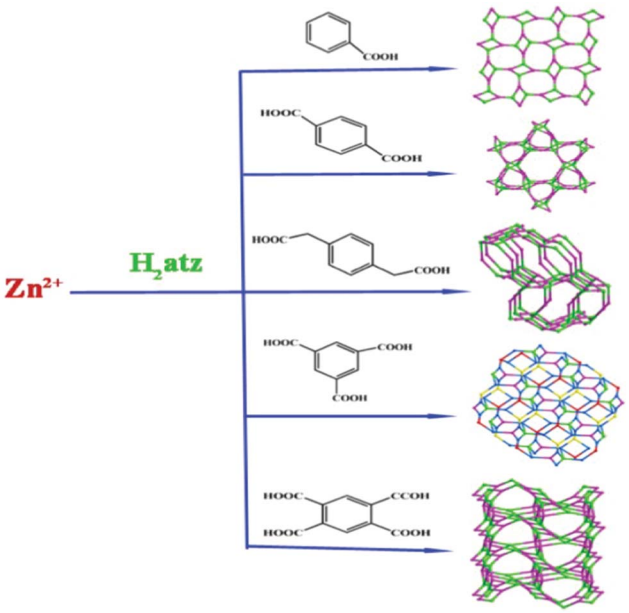

Scheme 1 Assembly of five Zn–atz compounds tuned by different carboxylate ligands.

and $\{[Zn_2(atz)_2(btec)]\cdot H_2O\}_n$ (**5**), (Hatz = 3-amino-1,2,4-triazolate Hbia = benzoic acid, H_2tpa = 1,4-terephthalic acid, H_2pda = 1,4-benzenediacetic acid, H_3btc = 1,3,5-benzenetricarboxylate, H_4btec = 1,2,4,5-benzenetetracarboxylic), have been successfully obtained under similar conditions. Their structures were determined by single-crystal X-ray diffraction analyses and further characterized by elemental analysis, infrared spectra (IR), thermogravimetric analysis (TGA) and powder X-ray diffraction (PXRD). On the basis of synthesis and structural characterization, the structural and topological analyses of these complexes as well as the effect of different aromatic carboxylates on the ultimate frameworks are discussed in detail, revealing that polycarboxylate ligand skeletons have a great influence on the architectures of MOFs and can be used as a tool to tune structures. In addition, the luminescence properties of complexes **1–5** have also been investigated in the solid state at room temperature.

Experimental section

Materials and general methods

All chemicals employed were commercially available and used as received without further purification. Elemental (C, H, N) analyses were performed on a Perkin-Elmer 2400 element analyzer. The Hatz ligand in compounds **1–3** was derived from the decarboxylation of 3-amino-1,2,4-triazole-5-carboxylic acid in the solvothermal process.[12] The FT-IR spectra were recorded from KBr pellets in the 4000–400 cm^{-1} ranges on a Nicolet 5DX spectrometer. Thermogravimetric analyses were performed on Perkin-Elmer TGA 7 analyzer with a heating rate of 10 °C min^{-1} in flowing air atmosphere. Luminescence spectroscopy data were recorded on an Edinburgh F900 FLS-900 spectrophotometer analyzer with a xenon arc lamp as the light source. In the measurements of emission and excitation spectra, the pass width is 5.0 nm. Powder X-ray diffraction (PXRD) patterns were recorded on a X-pert diffractometer or Rigaku D/M-2200T automated diffractometer for Cu Kα radiation (λ = 1.54056 Å), with a scan speed of 4° min^{-1} and a step size of 0.02° in 2θ range of 5–50°.

Synthesis of $\{[Zn(atz)(bia)]\}_n$ (1). A mixture of $ZnSO_4\cdot 6H_2O$ (143.8 mg, 0.5 mmol), 3-amino-1,2,4-triazole-5-carboxylic acid (38.5 mg, 0.3 mmol), Hbia (36.6 mg, 0.3 mmol) and water (10.0 mL) was placed in a 23 mL Teflon-lined stainless steel vessel. The pH value of the mixture was adjusted to 6 by triethylamine. The mixture was sealed and heated at 160 °C for three days, and then cooled to room temperature at a rate of 5 °C h^{-1}. White block-shaped crystals suitable for X-ray analysis were obtained with 76% yield based on Zn. Anal. calcd for $C_9H_8N_4ZnO_2$: C, 40.10; H, 2.30; N, 20.78%. Found: C, 40.12; H, 2.09; N, 20.77%. IR (cm^{-1}, KBr): 3387 (s), 3175 (m), 1607 (s), 1566 (s), 1395 (s), 1366 (m), 1307 (w), 1224 (m), 1077 (s), 853 (w), 718 (s), 688 (m), 647 (w).

Synthesis of $\{[Zn_3(atz)_3(tpa)_{3/2}]\}_n$ (2). The process was similar to **1** except that Hbia was replaced by H_2tpa (33.2 mg, 0.3 mmol). White block-shaped crystals suitable for X-ray analysis were obtained with 41% yield based on Zn. Anal. calcd for $C_{12}H_{10}N_8Zn_2O_7$: C, 28.31; H, 1.98; N, 22.01%. Found: C, 28.35; H, 2.02; N, 21.98%. IR (cm^{-1}, KBr): 3342 (s), 1643 (w), 1578 (s), 1407 (s), 1224 (m), 1042 (m), 883 (w), 836 (w), 753 (m).

Synthesis of $\{[Zn_2(atz)_2(pda)]\}_n$ (3). The process was similar to **1** except that Hbia was replaced by H_2pda (33.8 mg, 0.2 mmol). White block-shaped crystals suitable for X-ray analysis were obtained with 64% yield based on Zn. Anal. calcd for $C_{14}H_{14}N_8Zn_2O_4$: C, 34.38; H, 2.88; N, 22.91%. Found: C, 34.40; H, 2.87; N, 22.91%. IR (cm^{-1}, KBr): 3346 (s), 3175 (m), 2794 (w), 1596 (s), 1519 (w), 1366 (s), 1230 (m), 1060 (w), 947 (w), 883 (w), 794 (w), 729 (m), 653 (w), 602 (w).

Synthesis of $\{[Zn_4(atz)_2(btc)]\cdot 4H_2O\}_n$ (4). The process was similar to **1** except that Hbia was replaced by H_3btc (42 mg, 0.2 mmol). White crystals were obtained with 67% yield based on Zn.

Anal. calcd for $C_{22}H_{18}N_8Zn_4O_{15}$: C, 29.49; H, 2.02; N, 12.51%. Found: C, 29.51; H, 2.03; N, 12.50%. IR (cm^{-1}, KBr): 3410 (s), 3151 (m), 2974 (w), 1613 (s), 1578 (s), 1437 (s), 1366 (s), 1213 (w), 1048 (m), 883 (w), 729 (s), 619 (w).

Synthesis of $\{[Zn_2(atz)_2(btec)]\cdot H_2O\}_n$ (5). The process was similar to **1** except that Hbia was replaced by H_4btec (507 mg, 0.2 mmol). White crystals were obtained with 54% yield based on Zn. Anal. calcd for $C_{14}H_{12}N_8Zn_3O_{13}$: C, 24.14; H, 1.74; N, 16.09%. Found: C, 24.16; H, 1.73; N, 16.11%. IR (cm^{-1}, KBr): 3446 (m), 3351 (s), 2980 (w), 1585 (s), 1431 (m), 1389 (m), 1230 (m), 1048 (m), 883 (w), 847 (w), 806 (w), 594 (w).

Single-crystal structure determination

Data collections were performed at 298 K on a Bruker Smart Apex II diffractometer with graphite-monochromated Mo KR radiation (λ = 0.71073 Å) for complexes **1–5**. Absorption corrections were applied by using the multiscan program SADABS. Structural solutions and full-matrix least-squares refinements based on F^2 were performed with the SHELXS-97 and SHELXL-97 program packages, respectively.[13] All non-hydrogen atoms were refined anisotropically. The positions of hydrogen atoms were generated geometrically. The organic hydrogen atoms were placed in geometrically idealized positions and refined using a riding model. Hydrogen atoms attached to water molecules were located from difference Fourier maps and were also refined using a riding model. Details of the crystal parameters, data collections, and refinement for complexes **1–5** are summarized in Table 1. Hydrogen-bonding data for complexes **1** and **4** are listed in Table 2. Selected bond lengths and angles are shown in Table S1, ESI.† Further details are provided in ESI.†

Results and discussion

Structure of 1

The crystallographic analysis reveals that **1** crystallizes in the orthorhombic *Pbca* space group. The asymmetric unit consists of one unique Zn(II) atom, one atz ligand and one bia ligand. The Zn(II) ion adopts a distorted tetrahedron coordination environment, which is completed by three nitrogen atoms from three different atz ligands and one oxygen atom afforded by the monodentate bia ligand (Fig. 1a). The Zn–N distances range from 1.996(7) to 2.032(7) Å and the Zn–O distance is 2.020(10) Å. The bia ligand acts as an unexpected terminal coordinated ligand to construct the distorted tetrahedron geometry. The atz ligand adopts a $\mu_{1,2,4}$-bridging mode, two neighboring Zn(II) centers are connected by two pyrazole nitrogen atoms, forming a coplanar 6-membered hexagonal ring, and four symmetry-related Zn(II) centers are linked by four imidazole nitrogen atoms to fabricate a 16-membered non-planar chair-like ring. The interconnection of the two kinds of rings results in a 2D polymer network along the *ab* plane (Fig. 1b). On the basis of the topological approach of the simplification principle, the 2D polymer can be further simplified by considering that the atz ligand and Zn(II) center both act as 3-connected nodes with a (4.8^2) topological network (Fig. 1c). The uncoordinated oxygen atoms from bia ligands form hydrogen bonds with uncoordinated amino groups, which has significant impact on connecting the neighboring layers to generate a 3D supramolecular architecture in an –ABAB– fashion (Fig. 1d).

Structure of 2

To study the influence of the number of carboxylate groups on the complex structure, H_2tpa was selected in place of Hbia under similar synthetic conditions and a new complex **2** was obtained. Single-crystal X-ray diffraction analysis reveals that compound **2** crystallizes in the centrosymmetric tetragonal *P*4/*nnc* space group.

Table 1 Crystal data and structure refinement summary for compounds **1–5**

Complex	1	2	3	4	5
Empirical formula	$C_9H_8N_4ZnO_2$	$C_{12}H_{10}N_8Zn_2O_5$	$C_{14}H_{14}N_8Zn_2O_4$	$C_{22}H_{18}N_8Zn_4O_{15}$	$C_{14}H_{12}N_8Zn_3O_{13}$
Formula weight	269.58	477.06	489.11	896.00	696.49
T (K)	296(2)	296(2)	296(2)	296(2)	296(2)
Crystal system	Orthorhombic	Tetragonal	Monoclinic	Monoclinic	Monoclinic
Space group	*Pbca*	*P*4/*nnc*	$P2_1/c$	*C*2/*c*	*C*2/*c*
a (Å)	9.639(4)	12.700(3)	10.203(6)	22.579(3)	7.9770(9)
b (Å)	10.219(5)	12.700(3)	10.005(6)	18.542(3)	16.763(2)
c (Å)	21.866(10)	25.364(5)	18.287(10)	13.6018(19)	15.8519(19)
α (°)	90	90	90	90	90
β (°)	90	90	90.560(8)	92.614(2)	100.788(2)
γ (°)	90	90	90	90	90
V ($Å^3$)	2153.8(17)	4091(2)	1866.7(19)	5688.6(14)	2082.2(4)
Z	8	8	4	8	4
D_{calcd} ($g\ cm^{-3}$)	1.663	1.549	1.740	2.092	2.222
μ (mm^{-1})	2.270	2.383	2.609	3.424	3.521
F(000)	1088.0	1904.0	984.0	3568.0	1384.0
GOF	1.281	1.091	0.991	1.039	1.068
R_1 [$I > 2\sigma(I)$][a]	0.0775	0.0585	0.0655	0.0396	0.0781
wR_2 (all data)[b]	0.1818	0.1833	0.1860	0.1000	0.2009
Data/restraints/parameters	1977/12/145	1715/0/118	3013/0/253	5004/0/433	1835/611/169
CCDC number	917345	917346	917347	917348	917349

[a] $R_1 = \sum||F_o| - |F_c||/\sum|F_o|$. [b] $wR_2 = \{\sum[w(F_o^2 - F_c^2)^2]/\sum(F_o^2)^2\}^1$.

Table 2 Hydrogen bond lengths/Å and angles/° for **1–2**

Donor–H···Acceptor	*d*(D–H)	*d*(H···A)	∠DHA	*d*(D···A)
Compound **1**				
N4–H3···O2	0.86	2.01	150.1	2.789(16)
Compound **2**				
O2W–H2B···O12	0.85	1.78	173.6	2.620
O1W–H1A···O10	0.85	2.00	132.2	2.651(4)
O3W–H3A···O7	0.85	2.02	165.4	2.847(4)

The asymmetric unit of **2** includes one crystallographically independent Zn(II) atom, one tridentate atz ligand and one half tpa ligand (Fig. 2a). The Zn(II) atom has a slightly distorted tetrahedron geometry coordinated by three nitrogen atoms from three atz ligands and one oxygen atom from the carboxylate group of the tpa ligand. The Zn–N distances are ranging from 1.984(5) to 2.031(5) Å and the Zn–O distance is 1.947(5) Å. The structure of **2** is best described in terms of layers formed by the bridging atz ligand which presents the μ_3-1κN: 2κN: 4κN coordination mode (Fig. 2b). Such layers are further pillared by the aromatic backbones of tpa ligands to generate an overall 3D network (Fig. 2c). Furthermore, topological analysis is carried out for the complicated network of **2**. The Zn(II) atoms are simplified as 4-connected nodes, atz ligands as 3-connected nodes, and tpa ligands as lines, respectively. As a result, the 3D framework of **2** can be simplified as a 3,4-connected topology with Schläfli symbol $\{4.8^2.10^3\}\{4.8^2\}$ (Fig. 2d).

Structure of 3

Compared with complex **2**, the flexible H_2pda ligand was introduced in place of H_2tpa to investigate the role of flexible dicarboxylate ligands in the formation of Zn–atz polymers, and complex **3** was synthesized which exhibits a 3D entangled architecture and crystallizes in the monoclinic $P2_1/c$ space group with an asymmetric unit that contains two crystallographically independent Zn(II) ions, two atz ligands and one pda ligand (Fig. 3a). Both Zn1 and Zn2 ions are four-coordinated with distorted tetrahedron coordination geometries by three nitrogen atoms deriving from three distinct atz ligands, and one oxygen atom originating from a pda ligand. The Zn–N distances vary in the range of 1.977(5) to 2.048(5) Å, and the Zn–O bonds are 1.960(5) and 2.004(5) Å. Like compound **2**, the Zn(II) centers are linked by atz ligands to form a 1D chain along the *ab* plane. These 1D zigzag chains are connected by tpa ligands to form 2D layers (Fig. 3b). Furthermore, 2D layers are also linked by atz ligands to form a 3D framework (Fig. 3c). To further understand the structure, we define Zn(II) centers as 4-connected nodes, atz ligands as 3-connected nodes, and pda ligands as bridge linkers. Such 3D structures can be described in a 3,4-connected topology with Schläfli symbol $\{4.6.8\}\{4.6^2.8^3\}$ (Fig. 3d).

Structure of 4

Compared with the former complexes, H_3btc, which has three carboxylate groups, was introduced in place of H_2tpa to investigate the role of the number of carboxylate groups in the formation of Zn–trz polymers, then complex **4** was synthesized. Single-crystal X-ray crystallographic analysis reveals that **4** crystallizes in the monoclinic system with space group $P2_1/c$ and exhibits a 3D framework. The asymmetric unit of **4** is composed of four crystallographically independent Zn(II) centers, two dissimilar atz ligands, two btc ligands and three coordinated water molecules (Fig. 4). The four Zn(II) atoms are all in the tetrahedral

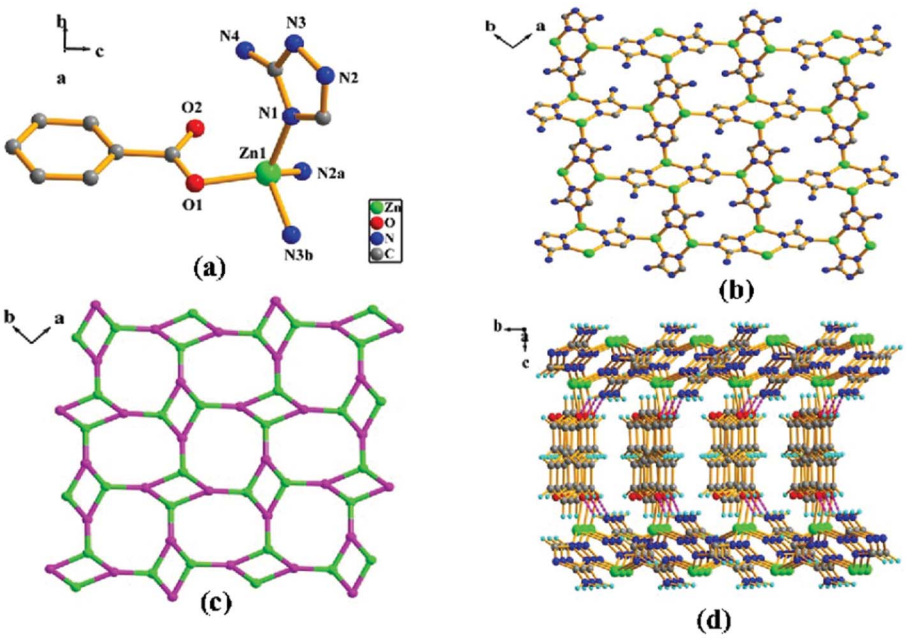

Fig. 1 (a) Coordination environment of complex **1**, all hydrogen atoms were omitted for clarity [symmetry code: a = 0.5 + *x*, 0.5 − *y*, 1 − *z*; b = 0.5 − *x*, −0.5 + *y*, *z*]; (b) a polyhedral view of the 2D layer structure constructed of 1D chains; (c) the topological (4.8^2) net of the 2D layer; (d) the supermolecular 3D framework constructed by intermolecular hydrogen bonds.

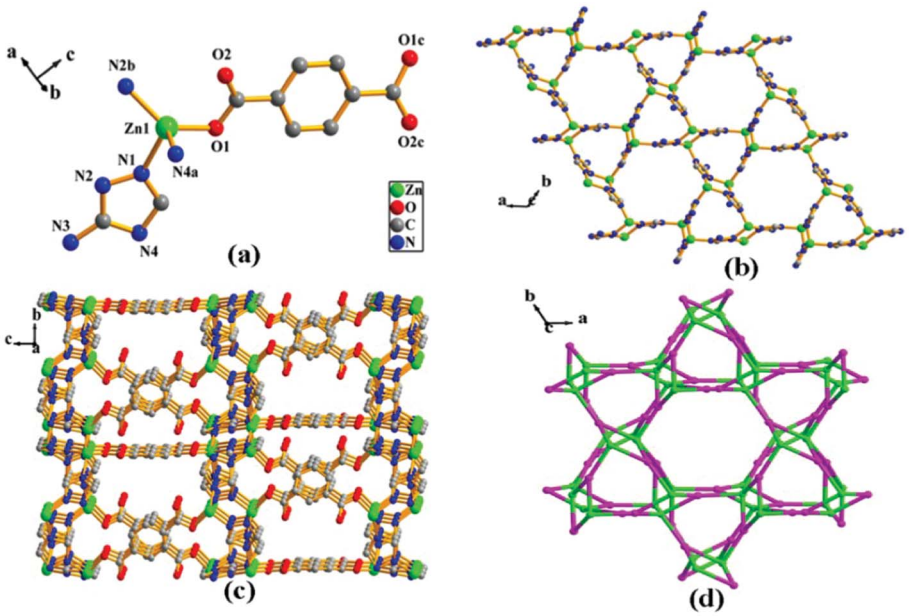

Fig. 2 (a) Coordination environment of complex **2**, all hydrogen atoms were omitted for clarity [symmetry code: a = −0.5 + *x*, 1 − *y*, 1 − *z*; b = 2 − *x*, −*y*, 1 − *z*; c = 1.5 − *x*, *y*, 1.5 − *z*]; (b) a polyhedral view of the 2D layer structure constructed of 1D chains; (c) the supermolecular 3D framework constructed by H_2tpa; (d) hexagon-like net with the topological notation $\{4.8^2.10^3\}\{4.8^2\}$. All amino groups were omitted for clarity in (b) and (c).

coordination geometry. Both Zn1 and Zn4 centers are coordinated to one nitrogen atom deriving from the atz ligand, two carboxylate oxygen atoms from two separate btc ligands, and one oxygen atom from the terminal coordinated water. While Zn2 is completed by two nitrogen atoms from two atz ligands, one oxygen atom from the monodentate carboxylate of btc ligand and one oxygen atom from the terminal coordinated water. Zn3 is surrounded by two nitrogen atoms from two atz ligands and two oxygen atoms afforded by two btc ligands. The Zn–N bond lengths vary from 1.977(4) to 1.999(4) Å, and Zn–O bond lengths vary from 1.910(3)

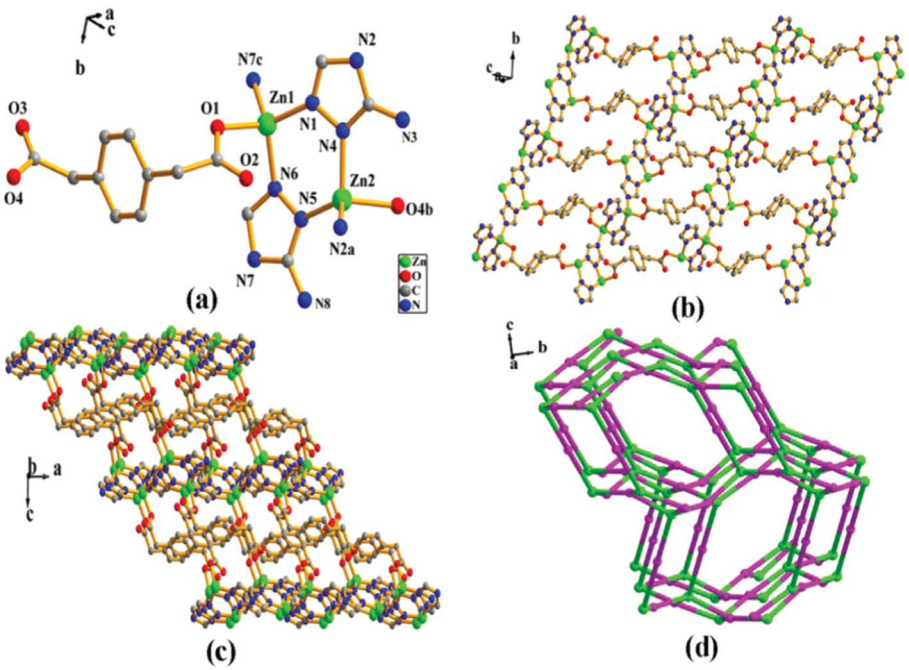

Fig. 3 (a) Coordination environment of complex **3**, all hydrogen atoms were omitted for clarity [symmetry code: a = 2 − *x*, 0.5 + *y*, 0.5 − *z*; b = 1 + *x*, 0.5 − *y*, 0.5 + *z*; c = 1 − *x*, −0.5 + *y*, 0.5 − *z*]; (b) a polyhedral view of the 2D layer structure constructed of 1D chains; (c) the supermolecular 3D framework constructed by H_2pda; (d) diamond-like net with Schläfli symbol $\{4.6.8\}\{4.6^2.8^3\}$. All amino groups were omitted for clarity in (b) and (c).

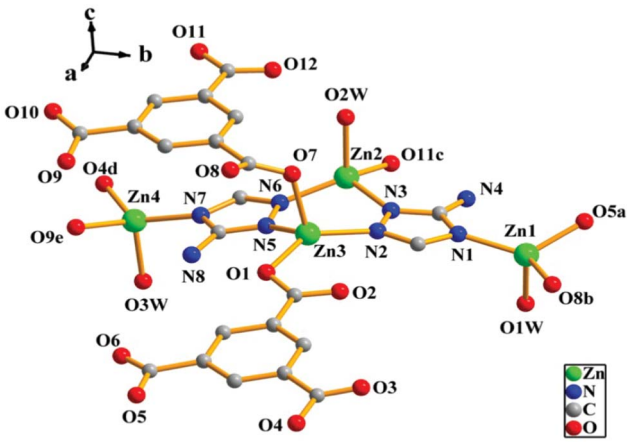

Fig. 4 Coordination environment of complex 4, all hydrogen atoms were omitted for clarity [symmetry code: $a = -0.5 + x, 0.5 + y, z$; $b = 0.5 - x, 0.5 - y, 1 - z$; $c = -x, -y, 1 - z$; $d = -0.5 + x, -0.5 + y, z$; $e = 0.5 - x, -0.5 - y, 1 - z$].

to 2.075(4) Å. All the atz ligands show uniform $\mu_{1,2,4}$-bridging modes, connecting Zn2 and Zn3 ions in the $\mu_{1,2}$-mode, Zn1 and Zn2 as well as Zn3 and Zn4 in $\mu_{1,4}$-modes, respectively. Each bta ligand links three Zn(II) centers through three carboxylate groups, then the Zn(II) centers are linked *via* btc and atz ligands into an infinite ziplike chain. Thus, the interconnection of the two kinds of chains results in a 2D polymeric network (Fig. 5a). It should be noted that the btc ligand can only link the adjacent two layers into an infinite 3D architecture by the monodentate carboxylate (Fig. 5b). To further understand the structure, topological analysis is performed on complex **4**, the Zn(II) centers are treated as 3 or 4-connected nodes, atz ligands as 3-connected nodes, and btc ligands as 3-connected nodes, the 3D structure can be described as 9-nodal net with a Schläfli symbol of $\{4.8.9\}_2\{4.8^2\}\{4.8^3.9.10\}\{5.8.9\}_4\{5.8^2\}$ (Fig. 5c). The infinite 3D architectures exhibit a layered arrangement, in which O–H–O type hydrogen bond interactions have been observed due to the interaction between the coordinated water molecules and uncoordinated carboxylato-oxygen atoms playing a key role in the supramolecular architecture (Fig. 5d).

Structure of 5

Single-crystal X-ray crystallographic analysis reveals that **5** crystallizes in the monoclinic system with the space group $P2_1/c$ and exhibits a 3D framework. The asymmetric unit of **5** contains two crystallographically independent Zn(II) atoms, two atz ligands, one completely deprotonated btec and one coordinated water (Fig. 6). It can be clearly seen that Zn1 is coordinated to two nitrogen atoms from symmetry-related atz ligands, and two oxygen atoms from symmetry-related carboxylate groups of two btec ligands, displaying a distorted tetrahedron geometry. While Zn2 displays a distorted octahedral coordination geometry, which is provided by two nitrogen atoms from two different atz ligands, and three oxygen atoms from two carboxylate groups of two btec ligands as well as one oxygen atom from a terminal coordinated water molecule. The atz ligand holds two Zn(II) ions together and is responsible for the formation of the 1D ribbon structure. These 1D ribbons are further extended by btec ligands to generate a 3D framework. The Zn–N bond lengths in the range of 1.973(7) to 2.031(6) Å, and the Zn–O bond lengths range from 1.966(7) to

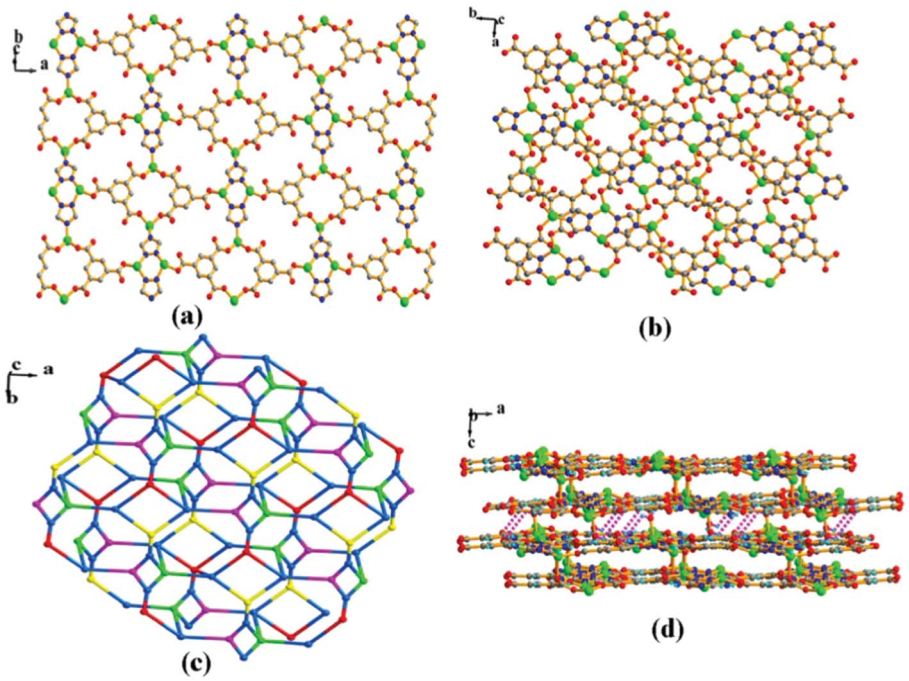

Fig. 5 (a) A polyhedral view of the 2D layer structure constructed of 1D chains for **4**; (b) two layers constructed by H_3btc; (c) 4-nodal (3,3,3,4)-connected framework with Schläfli symbol $\{4.8.9\}_2\{4.8^2\}\{4.8^3.9.10\}\{5.8.9\}_4\{5.8^2\}$, red: Zn1; pink: Zn2; green: Zn3; yellow: Zn4. (d) The supermolecular 3D framework constructed by hydrogen bonds. All amino groups were omitted for clarity in (a), (b) and (d).

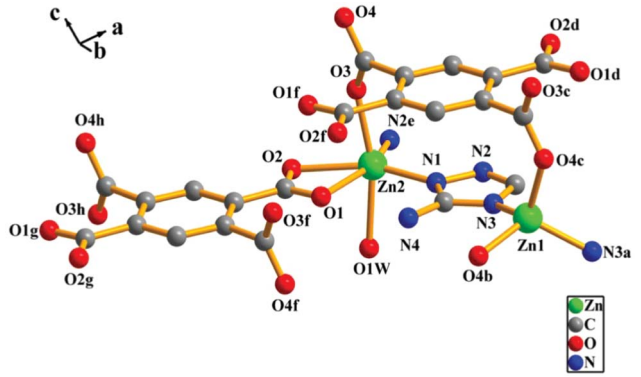

Fig. 6 Coordination environment of complex **5**, all hydrogen atoms were omitted for clarity [symmetry code: a =2 − *x*, *y*, 0.5 − *z*; b = *x*, −*y*, −0.5 + *z*; c = 2 − *x*, 1 − *y*, 1 − *z*; d = 1 + *x*, *y*, *z*; e = 1.5 − *x*, 0.5 − *y*, 1 − *z*; f = 1 − *x*, −*y*, 1 − *z*; *g* = −*x*, −*y*, 1 − *z*; h = −1 + *x*, *y*, *z*].

2.276(6) Å. The Zn(II) centers are linked by btec and atz ligands to form a infinite chain (Fig. 7a). These infinite chains are connected by atz ligands to form 2D layers (Fig. 7b). Furthermore, another two carboxylate groups of btec ligands show a chelate–bidentate fashion to connect the 2D layers to generate a 3D pillar-layered framework (Fig. 7c). In order to better understand the final architecture of the complex, the dinuclear Zn(II) unit, which is linked by carboxyl groups, can be defined Zn atoms as 4-connected nodes, atz ligands as 3-connected nodes, btec ligands as 4-connected nodes. In this way, the 3D structure can be described as 3,4,4-connected with a Schläfli symbol of $\{4.8^2\}_4\{4^2.8^3.10\}_2\{8^4.10^2\}$ (Fig. 7d).

Influence of carboxylates on the structures of the complexes

In light of the structure description, a novel family of Zn(II) compounds have been successfully synthesized under similar conditions except the used polycarboxylate ligands. On the basis of the X-ray analysis results, the crystal structures of these five compounds ranging from 2D layers to 3D coordination architectures indicate that the series of different polycarboxylate ligands are critical factors in the formation of such coordination architectures, and previous reports have mentioned the role of organic carboxylate anions.[14] Generally, the role of polycarboxylate ligands can be explained in terms of their differences in the number of carboxylate groups, the lengths of the spacer and the flexible abilities. Complexes **1** and **2** are mainly attributed to the effect of the spacer group of the carboxylate ligands, complex **1** is a 2D layer by using a bia ligand which has only one carboxylate group. When H_2tpa with a rigid spacer and an angle of 180° between the two carboxylic groups acting as a linker is introduced into the synthetic procedure, the 3D 4-connected structure of **3** is obtained. Complexes **2** and **3** imply the influence of the spacer length and flexibility of the carboxylate ligands on the resulting frameworks. Although both H_2tpa and H_2pda are based on benzene spacers, the length and flexibility of the spacers are different. H_2pda possesses flexibility owing to the presence of the –CH_2– spacer, which allows the two carboxylate groups to bridge the metals from different directions. Obviously, the structural difference of compounds **4** and **5** is mainly attributed to the different angles between the carboxylate groups in each ligand.

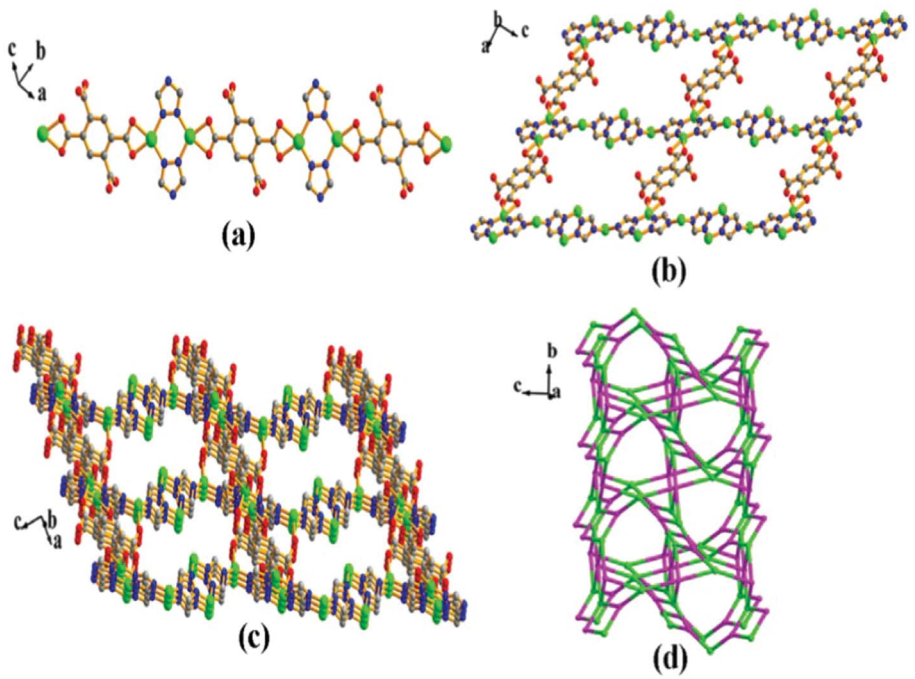

Fig. 7 (a) The Zn(II) centers are linked by btec and atz ligands to form an infinite chain for **5**; (b) the atz ligands as pillars to extend the 1D chains to be 2D net; (c) the supermolecular 3D framework constructed by H_4btec; (d) 4,4-connected framework with Schläfli symbol $\{4.8^2\}_4\{4^2.8^3.10\}_2\{8^4.10^2\}$. All amino groups were omitted for clarity in (a), (b) and (c).

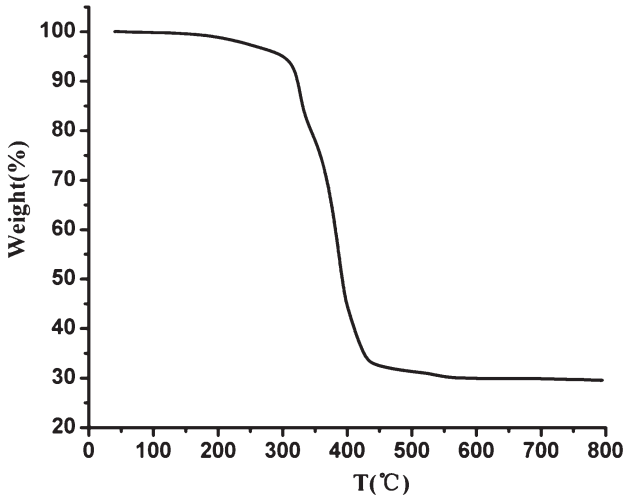

Fig. 8 TGA curve of compound **1**.

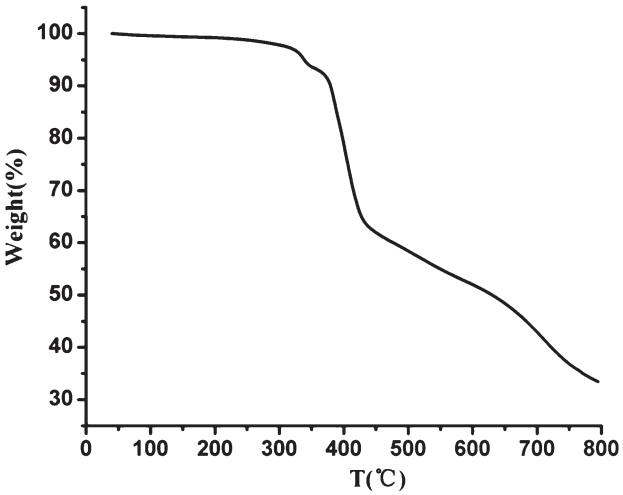

Fig. 10 TGA curve of compound **3**.

Thermal analysis and PXRD patterns

In order to characterize the complexes more fully in terms of thermal stability, TGA experiments were investigated on polycrystalline samples in the temperature range of 30–800 °C with a heating rate of 10 °C min^{-1} in dry air atmosphere (Fig. 8–12). For compounds **1** and **3**, no weight loss is observed until it reaches 320 and 310 °C, respectively, corresponding to the decomposition of the organic ligands. For compound **2**, the weight loss from 200 to 245 °C is consistent with the loss of three crystal-lattice water molecules (observed, 11.34%; calculated, 11.31%). Then no significant weight loss is observed until the decomposition of the framework occurs at 355 °C. Compound **4** undergoes two weight loss steps. The first weight loss is observed in the range of 120–225 °C, which is attributed to the release of three coordinated water molecules (observed, 5.98%; calculated, 6.03%), and then the decomposition of the ligands at 390 °C. The TGA curve of **5** shows a weight loss process under 225 °C, corresponding to the loss of free water molecules (observed, 7.72%; calculated, 7.75%), and then a plateau region follows until 390 °C. The further weight losses represent the decomposition of the ligands.

X-Ray powder diffraction (PXRD)

PXRD experiments were carried out for **1–5** to confirm whether the crystal structures are truly representative of the bulk materials (Fig. S1–S5, ESI†). By comparison, the experimental patterns and the simulated patterns are in good agreement with each other, which confirms the phase purity of the as-synthesized products.

Luminescent properties

Luminescent properties of compounds containing d^{10} metal centers are of intense interest due to their potential applications, such as in chemical sensors, photochemistry and electroluminescent display, and so on.[15] Hence, the solid-state luminescent properties of complexes **1–5**, together with the free Hatz ligand,

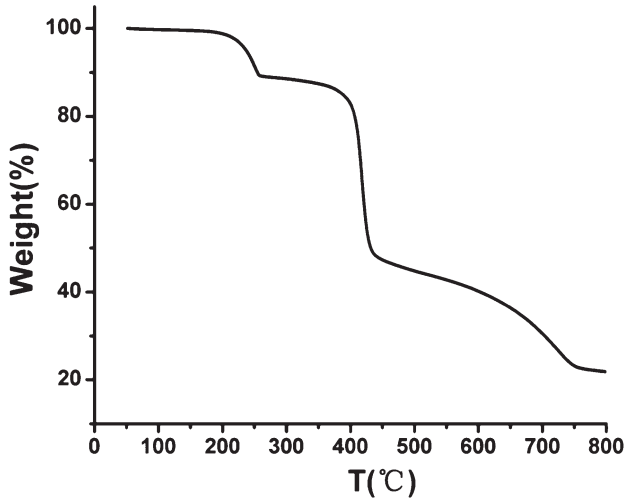

Fig. 9 TGA curve of compound **2**.

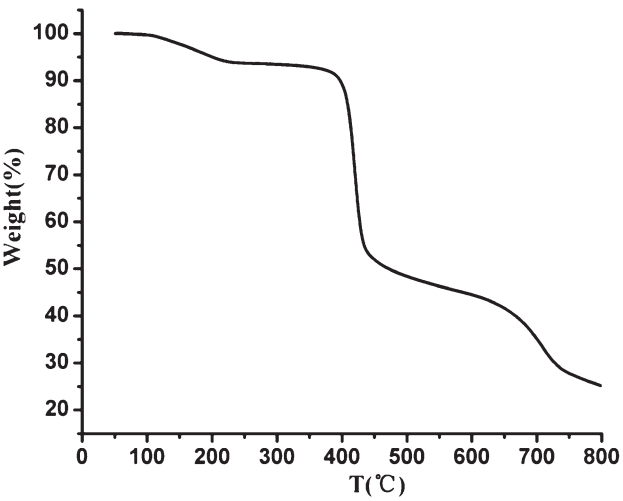

Fig. 11 TGA curve of compound **4**.

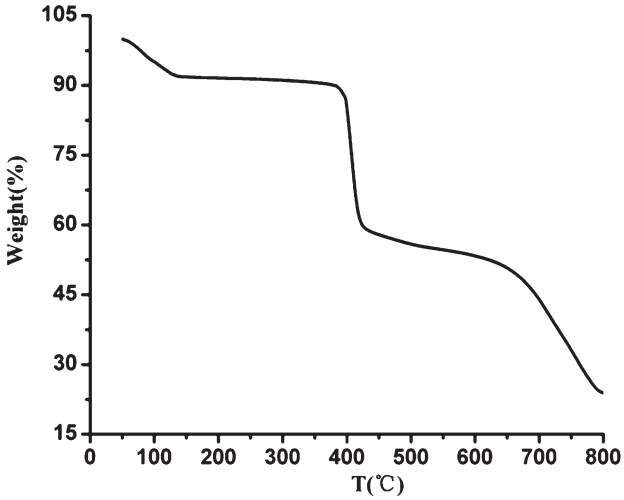

Fig. 12 TGA curve of compound **5**.

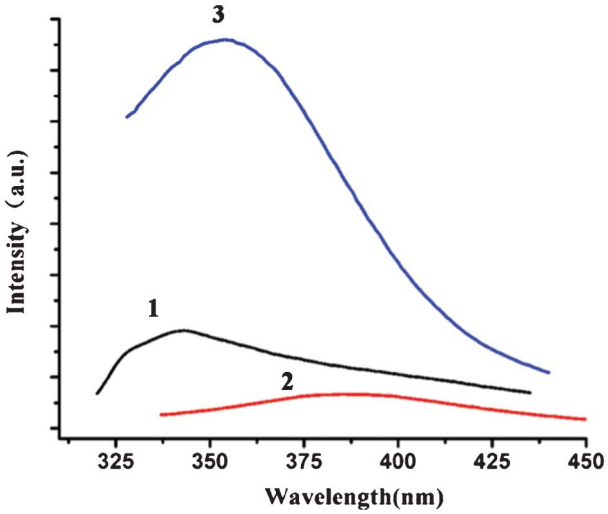

Fig. 14 Solid-state emission spectra at room temperature for **1**, **2**, **3**.

have been determined at room temperature (Fig. 13 and 14). The free ligand Hatz exhibits an emission band at 411 nm (λ_{ex} = 325 nm). Complexes **1–5** show broad emission bands with the maximum peak at 343 nm (λ_{ex} = 297 nm) for **1**, 385 nm (λ_{ex} = 314 nm) for **2**, 354 nm (λ_{ex} = 274 nm) for **3**, 421 nm (λ_{ex} = 327 nm) for **4** and 447 nm (λ_{ex} = 366 nm) for **5**. Compared with free Hatz ligand, the emissions for **1**, **2** and **3** are blue-shifted by 68 nm, 26 nm and 57 nm, respectively. The results may be attributed to intraligand luminescent emission, and the lightly blue-shifted may be attributed to the chelating of the Hatz ligand-to-metal charge transfer (LMCT), which effectively increases the rigidity of the ligand and reduces the loss of energy by radiationless decay of the intraligand emission excited state.[16] While the emissions for **4** and **5** are slightly red-shifted by 10 nm and 36 nm, respectively, which may be assigned to metal-to-ligand charge transfer (MLCT), and similar red shifts have been observed before.[17] From above discussion, all the complexes with the same Zn(II) center and N-donor ligand show different behaviors, which are probably attributed to the coordination environment around them and even the structural topologies. These compounds may be good blue-light emitting candidate materials, since they display luminescence in the blue region.[18]

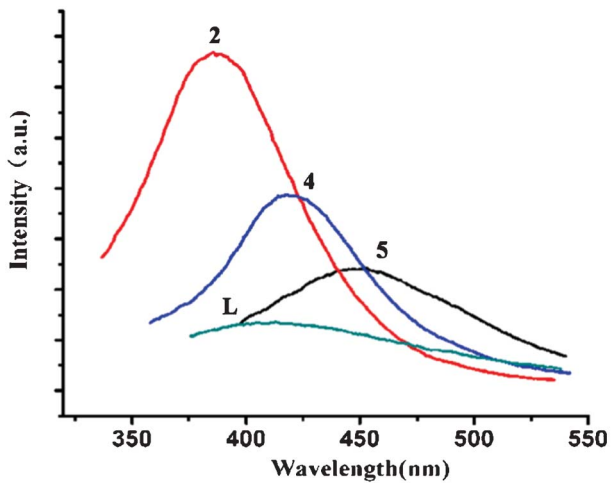

Fig. 13 Solid-state emission spectra at room temperature for **L**, **2**, **4**, **5**.

Conclusion

In summary, five novel coordination polymers of Zn(II)–atz have been successfully synthesized under hydrothermal reactions assisted with a series of auxiliary carboxylate ligands. They show diverse structures and dimensionalities from 2D network to 3D coordination architecture. This investigation demonstrates that the number of the carboxylate groups, the length and flexibility of carboxylate ligands play significant roles in constructing the structures of coordination polymers. Therefore, a new paradigm for further rational design and synthesis of new entangled MOFs can be accomplished by careful control of auxiliary ligands. The thermogravimetric analyses show that complexes **1–3** exhibit high thermal stability. Furthermore, their interesting luminescent behavior indicates that these complexes may be suitable as excellent candidates for optical materials.

Acknowledgements

We are thankful for financial support from NSFC (Grants 20971047, U0734005 and 21271076), and Key Research Program of Guangdong Provincial Universities Science and Technology innovation (Grant cxzd1020).

References

1 (*a*) M. O'Keeffe, M. H. Eddaoudi, L. Li, T. Reineke and O. M. Yaghi, *J. Solid State Chem.*, 2000, **152**, 3; (*b*) P. J. Hagrman, D. Hagrman and J. Zubieta, *Angew. Chem., Int. Ed.*, 1999, **38**, 2638; (*c*) B. Moulton and M. J. Zaworotko, *Chem. Rev.*, 2001, **101**, 1629; (*d*) Z. Y. Li, J. W. Dai, N. Wang, H. H. Qiu, S. T. Yue and Y. L. Liu, *Cryst. Growth Des.*, 2010, **10**, 2746; (*e*) M. Du, Z. H. Zhang and X. J. Zhao, *Cryst. Growth Des.*, 2006, **6**, 390.

2 (*a*) O. R. Evans and W. Lin, *Acc. Chem. Res.*, 2002, **35**, 511; (*b*) S. L. James, *Chem. Soc. Rev.*, 2003, **32**, 276; (*c*) J. Fu, H. Li, Y. Mu, H. Hou and Y. Fan, *Chem. Commun.*, 2011, **47**, 5271; (*d*) X. Shi, W. Wang, H. Hou and Y. Fan, *Eur. J. Inorg. Chem.*, 2010, **23**, 3652; (*e*) N. W. Ockwig, O. Delgado-Friedrichs, M. O'Keeffe and O. M. Yaghi, *Acc. Chem. Res.*, 2005, **38**, 176.

3 (*a*) M. F. Wu, M. S. Wang, S. P. Guo, F. K. Zheng, H. F. Chen, X. M. Jiang, G. N. Liu, G. C. Guo and J. S. Huang, *Cryst. Growth Des.*, 2011, **11**, 372; (*b*) L. Liang, G. Peng, L. Ma, L. Sun, H. Deng, H. Li and W. S. Li, *Cryst. Growth Des.*, 2012, **12**, 1151; (*c*) R. K. Chiang, N. T. Chuang, C. S. Wu, M. F. Chong and C. R. Lin, *J. Solid State Chem.*, 2002, **166**, 158; (*d*) W. Kaneko, S. Kitagawa and M. Ohba, *J. Am. Chem. Soc.*, 2007, **129**, 248.

4 (*a*) J. Park, D. Yuan, K. Pham, J. R. Li, A. Yakovenko and H. C. Zhou, *J. Am. Chem. Soc.*, 2012, **134**, 99; (*b*) Q. P. Lin, T. Wu, S. T. Zheng, X. H. Bu and P. Y. Feng, *J. Am. Chem. Soc.*, 2012, **134**, 784; (*c*) L. Pan, K. M. Adams, H. E. Hernandez, X. Wang, C. Zheng, Y. Hattori and K. Kaneko, *J. Am. Chem. Soc.*, 2003, **125**, 3062; (*d*) D. J. Collins and H. C. Zhou, *J. Mater. Chem.*, 2007, **17**, 3154.

5 (*a*) B. Xu, H. L. Guo, S. Wang, Y. Y. Li, H. J. Zhang and C. G. Liu, *CrystEngComm*, 2012, **14**, 2914; (*b*) X. H. Yan, Y. F. Li, Q. Wang, X. G. Huang, Y. Zhang, C. J. Gao, W. S. Liu, Y. Tang, H. R. Zhang and Y. L. Shao, *Cryst. Growth Des.*, 2011, **11**, 4205; (*c*) M. D. Allendorf, C. A. Bauer, R. K. Bhakta and R. J. T. Houk, *Chem. Soc. Rev.*, 2009, **38**, 1330; (*d*) X. Wang, W. Yao, Y. F. Qi, M. F. Luo, Y. H. Wang, H. W. Xie, Y. Yu, R. Y. Ma and Y. G. Li, *CrystEngComm*, 2011, **13**, 2542; (*e*) S. Q. Su, W. Chen, C. Qin, S. Y. Song, Z. Y. Guo, G. H. Li, X. Z. Song, M. Zhu, S. Wang, Z. M. Hao and H. J. Zhang, *Cryst. Growth Des.*, 2012, **12**, 1808.

6 (*a*) C. D. Wu, A. G. Hu, L. Zhang and W. B. Lin, *J. Am. Chem. Soc.*, 2005, **127**, 8940; (*b*) J. Wu, H. W. Hou, Y. X. Guo, Y. T. Fan and X. Wang, *Eur. J. Inorg. Chem.*, 2009, **19**, 2796; (*c*) F. X. L. I. Xamena, A. Abad, A. Corma and H. J. Garcia, *Catal.*, 2007, **250**, 294; (*d*) F. X. L. I. Xamena, O. Casanova, R. G. Tailleur, H. Garcia and A. J. Corma, *Catal.*, 2008, **255**, 220.

7 (*a*) P. Q. Zheng, Y. P. Ren, L. S. Long, R. B. Huang and L. S. Zheng, *Inorg. Chem.*, 2005, **44**, 1190; (*b*) L. F. Ma, L. Y. Wang, D. H. Lu, S. R. Batten and J. G. Wang, *Cryst. Growth Des.*, 2009, **9**, 1741; (*c*) C. P. Li and M. Du, *Chem. Commun.*, 2011, **47**, 5958; (*d*) C. M. Liu, S. Gao, D. Q. Zhang and D. B. Zhu, *Cryst. Growth Des.*, 2007, **7**, 1312; (*e*) J. G. Lin, Y. Y. Xu, L. Qiu, S. Q. Zang, C. S. Lu, C. Y. Duan, Y. Z. Li, S. Gao and Q. J. Meng, *Chem. Commun.*, 2008, **23**, 2659.

8 (*a*) Y. Q. Wei, Y. F. Yu and K. C. Wu, *Cryst. Growth Des.*, 2008, **8**, 2087; (*b*) W. G. Lu, L. Jiang and T. B. Lu, *Cryst. Growth Des.*, 2010, **10**, 4310; (*c*) W. J. Liu, Z. Y. Li, N. Wang, X. X. Li, Z. Q. Wei, S. T. Yue and Y. L. Liu, *CrystEngComm*, 2011, **13**, 138.

9 (*a*) A. X. Zhu, J. B. Lin, J. P. Zhang and X. M. Chen, *Inorg. Chem.*, 2009, **48**, 3882; (*b*) A. K. Paul, U. Sanyal and S. Natarajan, *Cryst. Growth Des.*, 2010, **10**, 4161.

10 (*a*) Y. W. Li, H. Ma, Y. Q. Chen, K. H. He, Z. X. Li and X. H. Bu, *Cryst. Growth Des.*, 2012, **12**, 189; (*b*) J. Xu, W. P. Su and M. C. Hong, *Cryst. Growth Des.*, 2011, **11**, 337; (*c*) F. Nouar, J. Eckert, J. F. Eubank, P. Forster and M. Eddaoudi, *J. Am. Chem. Soc.*, 2009, **131**, 2864.

11 (*a*) E. C. Yang, Z. Y. Liu, X. J. Shi, Q. Q. Liang and X. J. Zhao, *Inorg. Chem.*, 2010, **49**, 7969; (*b*) R. Q. Fang, X. H. Zhang and X. M. Zhang, *Cryst. Growth Des.*, 2006, **6**, 2637; (*c*) R. B. Zhang, Z. J. Li, Y. Y. Qin, J. K. Cheng, J. Zhang and Y. G. Yao, *Inorg. Chem.*, 2008, **47**, 4861.

12 (*a*) C. Y. Su, A. M. Goforth, M. D. Smith, P. J. Pellechia and H. C. Zurloye, *J. Am. Chem. Soc.*, 2004, **126**, 3576; (*b*) S. P. Chen, S. Sun and S. L. Gao, *J. Solid State Chem.*, 2008, **181**, 3308; (*c*) Z. L. Chen, X. L. Li and F. P. Liang, *J. Solid State Chem.*, 2008, **181**, 2078.

13 (*a*) G. M. Sheldrick, *SHELXL97*, Germany, 1997; (*b*) D. Santamaria-Perez, A. Vegas, C. Mühle and M. Jansen, *Acta Crystallogr., Sect. B: Struct. Sci.*, 2011, **67**, 109; (*c*) *Bruker, APEX II, SAINT*, Bruker AXS Inc., Madison, Wisconsin, USA, 2004.

14 (*a*) B. H. Ye, M. L. Tong and X. M. Chen, *Coord. Chem. Rev.*, 2005, **249**, 545; (*b*) J. P. Zhao, B. W. Hu, Q. Yang, T. L. Hu and X. H. Bu, *Inorg. Chem.*, 2009, **48**, 7111.

15 (*a*) W. Ouellette, B. S. Hudson and J. Zubieta, *Inorg. Chem.*, 2007, **46**, 4887; (*b*) C. M. Che, H. Y. Chao, V. M. Miskowski, Y. Q. Li and K. K. Cheung, *J. Am. Chem. Soc.*, 2001, **123**, 4985; (*c*) X. He, C. Z. Lu and D. Q. Yuan, *Inorg. Chem.*, 2006, **45**, 5760; (*d*) Q. Wu, M. Esteghamatian, N. X. Hu, Z. Popovic, G. Enright, Y. Tao, M. D'Iorio and S. Wang, *Chem. Mater.*, 2000, **12**, 79; (*e*) J. E. McGarrah, Y. J. Kim, M. Hissler and R. Eisenberg, *Inorg. Chem.*, 2001, **40**, 4510.

16 (*a*) X. M. Zhang, M. L. Tong, M. L. Gong and X. M. Chen, *Eur. J. Inorg. Chem.*, 2003, **1**, 138; (*b*) L. Y. Zhang, G. F. Liu, S. L. Zheng, B. H. Ye, X. M. Zhang and X. M. Chen, *Eur. J. Inorg. Chem.*, 2003, **16**, 2965; (*c*) X. D. Guo, G. S. Zhu, F. X. Sun, Z. Y. Li, X. J. Zhao, X. T. Li, H. C. Wang and S. L. Qiu, *Inorg. Chem.*, 2006, **45**, 2581.

17 X. Shi, G. Zhu, Q. Fang, G. Wu, G. Tian, R. Wang, D. Zhang, M. Xue and S. Qiu, *Eur. J. Inorg. Chem.*, 2004, **1**, 185.

18 H. Y. Liu, H. Wu, J. F. Ma, Y. Y. Liu, B. Liu and J. Yang, *Cryst. Growth Des.*, 2010, **10**, 4795.

